JOURNAL OF VIROLOGY, Apr. 1994, p. 2320–2330
0022-538X/94/$04.00+0

Vol. 68, No. 4

Effects of Provirus Integration in the *Tpl-1/Ets-1* Locus in Moloney Murine Leukemia Virus-Induced Rat T-Cell Lymphomas: Levels of Expression, Polyadenylation, Transcriptional Initiation, and Differential Splicing of the *Ets-1* mRNA

ALFONSO BELLACOSA,[1]† KETAKI DATTA,[1] SUSAN E. BEAR,[1] CHRISTOS PATRIOTIS,[1] PEDRO A. LAZO,[1]‡ NEAL G. COPELAND,[2] NANCY A. JENKINS,[2] AND PHILIP N. TSICHLIS[1]*

Fox Chase Cancer Center, Philadelphia, Pennsylvania 19111,[1] and ABL-Basic Research Program, National Cancer Institute—Frederick Cancer Research and Development Center, Frederick, Maryland 21702[2]

Received 28 July 1993/Accepted 13 December 1993

The *Tpl-1* locus was defined as a genomic DNA region which is targeted by provirus insertion during progression of Moloney murine leukemia virus-induced rat T-cell lymphomas. Using a panel of 156 (*Mus musculus* × *Mus spretus*) × *Mus musculus* interspecific backcross mice, we mapped *Tpl-1* to mouse chromosome 9 at a distance of 1.2 ± 0.9 centimorgans from the *Ets-1* proto-oncogene (S. E. Bear, A. Bellacosa, P. A. Lazo, N. A. Jenkins, N. G. Copeland, C. Hanson, G. Levan, and P. N. Tsichlis, Proc. Natl. Acad. Sci. USA 86:7495–7499, 1989). In this report, we present evidence that all the known *Tpl-1* provirus insertions occurred immediately 5′ of the first exon of *Ets-1* (exon A) and that the earlier detected distance between *Tpl-1* and *Ets-1* was due to the high frequency of meiotic recombination in the region between the site of provirus integration and exon III. Northern (RNA) blot analysis of polyadenylated RNA from normal adult rat tissues and Moloney murine leukemia virus-induced T-cell lymphomas and hybridization to a *Tpl-1/Ets-1* probe derived from the 5′ end of the gene revealed two lymphoid cell-specific RNA transcripts, of 5.5 and 2.2 kb. Sequence analysis of a near-full-length (4,991-bp) cDNA clone of the 5.5-kb RNA revealed a 441-amino-acid open reading frame encoding a protein identical to the human and mouse Ets-1 proteins with the exception of five and nine species-specific conservative amino acid differences, respectively. The steady-state level of the *Tpl-1/Ets-1* RNA and of the Ets-1 protein was modestly elevated in tumors carrying a provirus in the *Tpl-1* locus. The relative ratio of the two *Ets-1* transcripts, which were shown to arise by differential polyadenylation, was not affected by provirus insertion. Moreover, the major site of transcriptional initiation, which was localized by primer extension 250 bp upstream of the 5′ end of the *Ets-1* cDNA clone, was shown to be identical in normal cells and tumors carrying a provirus in the *Tpl-1* locus. Finally, the differential splicing of *Ets-1* exon VII was shown by RNase protection to occur at a rate of 15 to 26% and to remain unaffected by provirus insertion. The subtlety of these effects, in contrast to the strong growth selection of cells with a provirus in the *Tpl-1/Ets-1* locus, suggests that provirus insertion may affect the fine regulation of the gene, perhaps during cell cycle progression.

Insertional mutagenesis is the single most important factor responsible for the induction and progression of retrovirus-induced neoplasms. The effects of provirus integration vary depending on the precise location of the site of insertion relative to the targeted gene. Thus, in some cases the 5′ or 3′ end of the targeted gene may be altered by truncation and fusion between cellular and viral sequences. In many cases these alterations affect only the 5′ or 3′ untranslated region of the targeted gene, whereas in others they disrupt the coding sequences as well, thus altering the encoded protein product. Finally, in most cases the overall level of expression of the targeted gene is enhanced (29).

Although in many cases provirus integration exerts a clearly defined effect on the expression or the structure, or both, of the targeted gene, in some cases it does not. For example, provirus insertion near c-*myc* and *Spi-1* usually does not affect either the structure or the level of expression of the RNA transcribed from these genes (18, 23). The paradox of clonal selection of cells carrying a provirus in these loci in the absence of detectable effects on gene expression has not been adequately explained to date. One explanation offered for c-*myc* is that provirus insertion affects promoter usage. The implication is that the c-*myc* RNA transcribed from the gene targeted by the provirus harbors a different 5′-end region, which may alter the efficiency of translation (23).

The studies described in this report were undertaken to determine the linkage between the *Tpl-1* locus and the *Ets-1* proto-oncogene as well as the effects of provirus integration in the *Tpl-1* locus. Our earlier studies had shown that *Tpl-1* is localized on mouse chromosome 9 at a distance of 1.2 ± 0.9 centimorgans from *Ets-1*. The same studies had shown that provirus integration in this locus occurs during tumor progression and that cells harboring this genetic change are rapidly selected (1). In this report we show that all the known *Tpl-1* provirus insertions occurred immediately 5′ of the first exon of *Ets-1* (exon A) and that the earlier detected distance between *Tpl-1* and *Ets-1* was due to the high frequency of meiotic

* Corresponding author.
† Present address: Institute of Medical Genetics, Catholic University Medical School, 00168 Rome, Italy.
‡ Present address: Institudo de Salud Carlos III, Madrid, Spain.

recombination between the site of proviral integrations and exon III. (The first exon of *Ets-1* in mammals is called exon A, whereas the second exon is called exon III [see references 12 and 33 for details].) Moreover, the rapid selection of these cells occurs in the absence of a significant change in the steady-state levels of the *Ets-1* mRNA and of the Ets-1 protein. Finally, we show that the structure of the *Ets-1* mRNA, as determined by the ratio of transcripts generated by differential polyadenylation, differential splicing, and promoter usage, remains unchanged. To reconcile the apparent rapid selection of cells with a provirus in the *Tpl-1/Ets-1* locus with the absence of clearly detectable effects on the expression of *Ets-1*, we propose that provirus insertion in this locus may affect the fine regulation of the gene, perhaps during cell cycle progression.

MATERIALS AND METHODS

Tissues, thymic lymphomas, and cell lines. Normal tissues were obtained from 4- to 6-week-old F344 rats. Thymic lymphomas were induced in Osborn-Mendel and Long-Evans rats by intraperitoneal inoculation with 5×10^5 PFU of Moloney murine leukemia virus (MoMuLV) at birth (30, 31). The cell lines were established from primary tumors (14). (The establishment of the cell lines in culture was preceded in many cases by the passage of the primary tumor cells in nude mice. The name of each cell line includes a number which identifies the animal from which the tumor was derived, followed by a notation indicating the passage history of the cells in nude mice. Thus, 2772T→As is a cell line which was established from the ascite developed in nude mice inoculated intraperitoneally with 2772 thymoma cells; 2772T→S was established from the tumor cells grown in the spleen of the nude mice; 2772T→Ln→Ln derived from the tumor cells grown in the lymph nodes of the nude mice [two passages]. 2772T→PP originated from the tumor cells grown in the Peyer's patches of the nude mice.)

Southern blot analysis of genomic DNA and genomic DNA cloning. Genomic DNA isolation and Southern blotting were carried out by standard procedures (30, 31). Hybridization of the pSB1 and *Ets-1* exon III and IX probes to mouse DNA was carried out under conditions of reduced stringency (40% formamide plus 6× SSC [1× SSC is 0.15 M NaCl plus 0.015 M sodium citrate] at 37°C). The filters hybridized under these conditions were washed three times with 2× SSC–0.1% sodium dodecyl sulfate (SDS) at room temperature and once with 1× SSC–0.1% SDS at 65°C for 30 min. Genomic DNA cloning was performed as previously described with a *Hae*III partial-digest rat genomic DNA library in bacteriophage λ Charon 4A (Clontech). The library was screened with the pSB1 probe, and two overlapping lambda clones, λTpl-1.6 and λTpl-1.21, were isolated.

Isolation of RNA, size selection, and Northern blot analysis. Total RNA was extracted from normal rat organs and MoMuLV-induced T-cell lymphoma lines by the guanidinium isothiocyanate-cesium chloride method (4). Polyadenylated RNA was selected by oligo(dT)-cellulose affinity chromatography (11). Polyadenylated RNA was size fractionated in a sucrose gradient as previously described (17). Northern (RNA) blot analysis was carried out by standard procedures (25). Briefly, 5 μg of polyadenylated RNA was electrophoresed in 1% agarose–2.2 M formaldehyde gels, transferred to nylon membranes (Hybond N; Amersham), and hybridized to the pSB8 and ribosomal protein L32 probes, probes A and B, under high-stringency conditions. The intensity of the bands was quantitated with a β scanner (AMBIS).

Western blotting. Extracts of T-cell lymphoma lines were prepared in RIPA buffer (50 mM Tris-HCl [pH 7.4], 150 mM NaCl, 1% Triton X-100, 0.1% SDS, 1% sodium deoxycholate, 1 mM sodium vanadate) containing protease inhibitors (1 mM phenylmethylsulfonyl fluoride, 10 μg of aprotinin per ml, 10 μg of leupeptin per ml). Total protein (75 μg) was subjected to SDS-polyacrylamide gel electrophoresis (PAGE) (10% polyacrylamide) and then transferred to a polyvinylidene difluoride membrane (Immobilon P; Millipore) with a semidry electroblotter (Millipore) at 2 mA/cm^2 for 1 h. Following staining with Ponceau Red to check for completion of the transfer, the membrane was blocked in 4% bovine serum albumin and probed with rabbit polyclonal antibody anti-Ets-1 (Santa Cruz Biotechnology). The signal was detected by an enhanced chemiluminescence method (ECL; Amersham). The intensity of the Ets-1 bands was evaluated with an image analyzer (AMBIS) coupled to a transilluminator (Photodyne).

Construction and screening of cDNA libraries. Oligo(dT)-primed cDNA was synthesized from 5 μg of unfractionated or size-selected polyadenylated RNA. Double-stranded cDNA, generated by the method of Gubler and Hoffman (8), was ligated to *Eco*RI linkers and inserted in the *Eco*RI arms of bacteriophage λZapII (Stratagene). Following in vitro packaging, the resulting mixture of recombinant phage particles was propagated in *Escherichia coli* XL-1 Blue. The library was screened with the pSB8 probe, and the isolated λ clones were directly subcloned in pBluescript SK(−) by in vivo excision (27). Two cDNA libraries were constructed; one was constructed from polyadenylated RNA derived from the tumor cell line 2772T→S, which contains a provirus in the *Tpl-1* locus (1), and the second was constructed from size-fractionated RNA (17) derived from tumor cell line 6889.

DNA sequence analysis; computer comparisons. The pRCT14a clone was sequenced as previously described (3). Briefly, nested deletions were generated in both directions by using the exonuclease III-mung bean nuclease method (10). Twenty plasmid clones with overlapping deletions starting at the 5′ end of pRCT14a and nineteen clones with overlapping deletions starting at the 3′ end were sequenced. The sequencing reactions were carried out on alkali-denatured double-stranded DNA (16) by using the dideoxy-chain termination method (26) and employing Sequenase version 2.0 (U.S. Biochemicals) and [α-^{35}S]dATP (NEN DuPont). G+C-rich areas were resolved by sequencing single-stranded DNA or by using dITP or both. The reactions were analyzed on 4 and 6% polyacrylamide–8.3 M urea sequencing gels. The sequences of genomic *Tpl-1* clones and of six clones isolated from the size-selected 6889 cDNA library were determined similarly. The GenBank data base was screened with the pRCT14a sequence by using the program Wordsearch. Comparisons between rat, human, and mouse *Ets-1* nucleotide and amino acid sequences were conducted with the program Bestfit. The same program was used to align the sequence of pRCT14a and the six size-selected cDNA clones. Wordsearch and Bestfit are part of the Genetics Computer Group software package (7).

PCR. *Ets-1/Tpl-1* exon-specific probes were generated by PCR (24). The following pairs of primers were used: exon III, 5′-gcgcgcgaattcATATGGAATGCGCAGAT-3′ and 5′-gcgcgc ctgcagCTTTGGGGATTCCCAGTC-3′; exon IX, 5′-gcgcgc gaattcGTGGCCAGGAGATGGGGA-3′ and 5′-ggaggactgcag TTACTCATCAGCATCCGG3′ (the exon sequences are shown in capital letters;moreover, the sequences of *Eco*RI and *Pst*I sites, introduced to allow cloning into pBluescript, are underlined). PCR reactions contained 50 pmol of each primer, 1 ng of template pRCT14a, standard buffers, and *Taq* polymerase (Perkin-Elmer Cetus). The PCR cycles consisted of a 1-min denaturation at 95°C, a 1-min annealing at 50°C and a

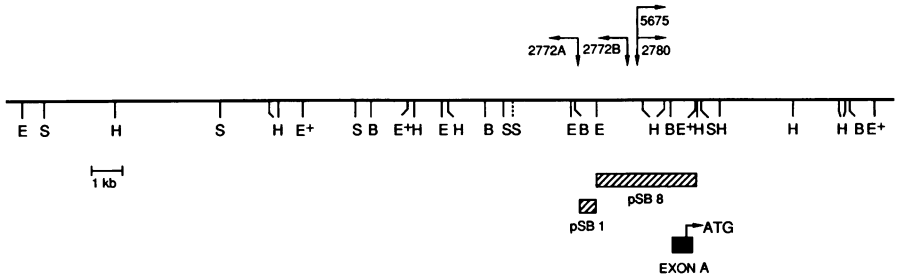

FIG. 1. Restriction map of the *Tpl-1* locus, depicting the origin of the probes pSB1 and pSB8, as well as the position and transcriptional orientation of the first exon (exon A) of the *Tpl-1/Ets-1* proto-oncogene. The arrows indicate the sites of insertion and orientation of the integrated proviruses in four primary tumors and cell lines (1). E, *Eco*RI; B, *Bam*HI; H, *Hin*dIII; S, *Sst*I. E^+ indicates artificial *Eco*RI sites, marking the end of genomic *Tpl-1/Ets-1* λ clones. The dotted line marks a polymorphic *Sst*I site.

1.5-min elongation at 72°C. PCR amplifications were carried out for 30 cycles in an M. J. Research thermal cycler.

Primer extension. Primer extension analysis was performed as previously described (2). Briefly, 10 μg of total RNA from normal rat thymus and the 2780 lymphoma line, which contains a provirus in the *Tpl-1* locus, was hybridized to 5 pmol of primer PT194 or PT265 (see Fig. 7), previously labeled at the 5′ end with [γ-^{32}P]ATP (ICN) and T4 polynucleotide kinase. Hybridization was carried out in 80% formamide at 30°C for 16 h. The primer-RNA hybrids were incubated with 100 U of MoMuLV reverse transcriptase at 37°C for 2 h. The single-stranded portions of the RNA were removed with DNase-free RNase (Sigma). The products of these reactions were electrophoresed in 6% polyacrylamide–8.3 M urea gels along with end-labeled DNA markers and sequencing reactions of genomic DNA using the same primers.

RNase protection. RNase protection assays were carried out by standard procedures (25). Briefly, a 334-bp *Sph*I-*Pst*I fragment spanning exons VI and VII (see Fig. 2) was subcloned in pGEM3Z. After linearization with *Hin*dIII, the construct was transcribed with T7 RNA polymerase (Promega) in vitro, as recommended by the manufacturer, by using [α-^{32}P]CTP (NEN DuPont). A 382-base riboprobe, which included 48 bases of vector sequences, was generated. The riboprobe (10^6 cpm per sample) was hybridized, in a solution containing 80% formamide, to total RNA (10 μg) at 63°C for 16 h and then digested with 40 μg of RNase A (Sigma) per ml. The products of the reaction were electrophoresed in 6% polyacrylamide–8.3 M urea gels along with end-labeled DNA markers. The intensity of the bands was quantitated with a β scanner.

Nucleotide sequence accession numbers. The sequences reported in this paper have been submitted to GenBank under accession numbers L20681, L20682, L21899, L21900, and L21901.

RESULTS

Screening a rat liver genomic DNA library with probe pSB1, which flanks the *Tpl-1* integrated provirus in the cell line 2772T→S, yielded two genomic DNA clones, λTpl-1.6 and λTpl-1.21 (Fig. 1) (1). Northern blots of 2772T→S polyadenylated RNA hybridized to the pSB8 probe, derived from these clones (Fig. 1), detected two mRNAs of approximately 5.5 and 2.2 kb. Using the pSB8 genomic probe to screen a cDNA library prepared from poly(A)$^+$ RNA derived from these cells yielded three cDNA clones, the largest of which (pRCT14a) was approximately 5 kb long.

Sequence analysis revealed that pRCT14a contained a 441-amino-acid open reading frame encoding a protein which was identical to the protein products of the human (32) and mouse (9) *Ets-1* proto-oncogenes, with the exception of five and nine conservative amino acid differences, respectively (Fig. 2). The differences between the rat and human proteins do not overlap with the differences between the rat and mouse proteins, suggesting that these differences are species specific and not tumor specific.

Earlier studies based on the frequency of recombination between genetic markers in (*Mus musculus* × *Mus spretus*) × *Mus musculus* interspecific backcross mice had shown that the *Tpl-1* locus maps to mouse chromosome 9 (1). The genetic distance between the DNA sequences recognized by the *Tpl-1* probe pSB1 and *Ets-1* exon VII was estimated to be ~1.2 ± 0.9 centimorgans (2 recombinants from 161 mice tested) (1). The earlier reported distance between *Tpl-1* and *Ets-1* and the conflicting finding of near identity between them, reported here, raised questions about the identity of *Tpl-1*. To address these questions, we first hybridized an *Eco*RI-*Xma*I probe derived from the 5′ untranslated region of the *Tpl-1/Ets-1* cDNA clone pRCT14a (Fig. 2) to a panel of MoMuLV-induced rat T-cell lymphoma DNAs digested with *Sst*I. The probe detected a single-copy sequence in normal rat DNA; this sequence was rearranged in tumors harboring a provirus in *Tpl-1* (Fig. 3A). Assuming that pRCT14a is a cDNA clone of *Ets-1* and not a cDNA clone of an *Ets-1*-related gene, this result suggested that *Tpl-1* is indeed *Ets-1* and that the apparent genetic distance between them is due to an unusually high frequency of intragenic recombination. To map the site of recombination, a pSB1 probe and a mixture of exon III and IX probes generated by PCR amplification, using exon-specific primers and pRCT14a as template, were hybridized to a panel of (*Mus musculus* × *Mus spretus*) × *Mus musculus* interspecific backcross mouse DNAs. This analysis revealed that two mice (mice 76 and 116) were homozygous for the *Mus musculus* pSB1 allele (Fig. 3B) and heterozygous for exons III and IX *Mus musculus* and *Mus spretus* alleles (Fig. 3C). This is compatible with a recombination event in the region between pSB1, located 2.5 kb 5′ of exon A, and exon III. The physical distance between these two markers is approximately 30 kb (12).

Provirus insertion in the *Tpl-1* locus occurred in primary tumors as well as in tumor cell lines maintained in culture, suggesting that the growth selection associated with provirus insertion in this locus operates both in vivo and in culture. Monitoring of T-cell lymphoma lines maintained in culture for provirus insertion in the *Tpl-1* locus revealed that once cells with *Tpl-1* rearrangements become detectable, approximately 24 cell divisions are sufficient to allow their clonal selection (1). We therefore proceeded to examine the molecular basis of this

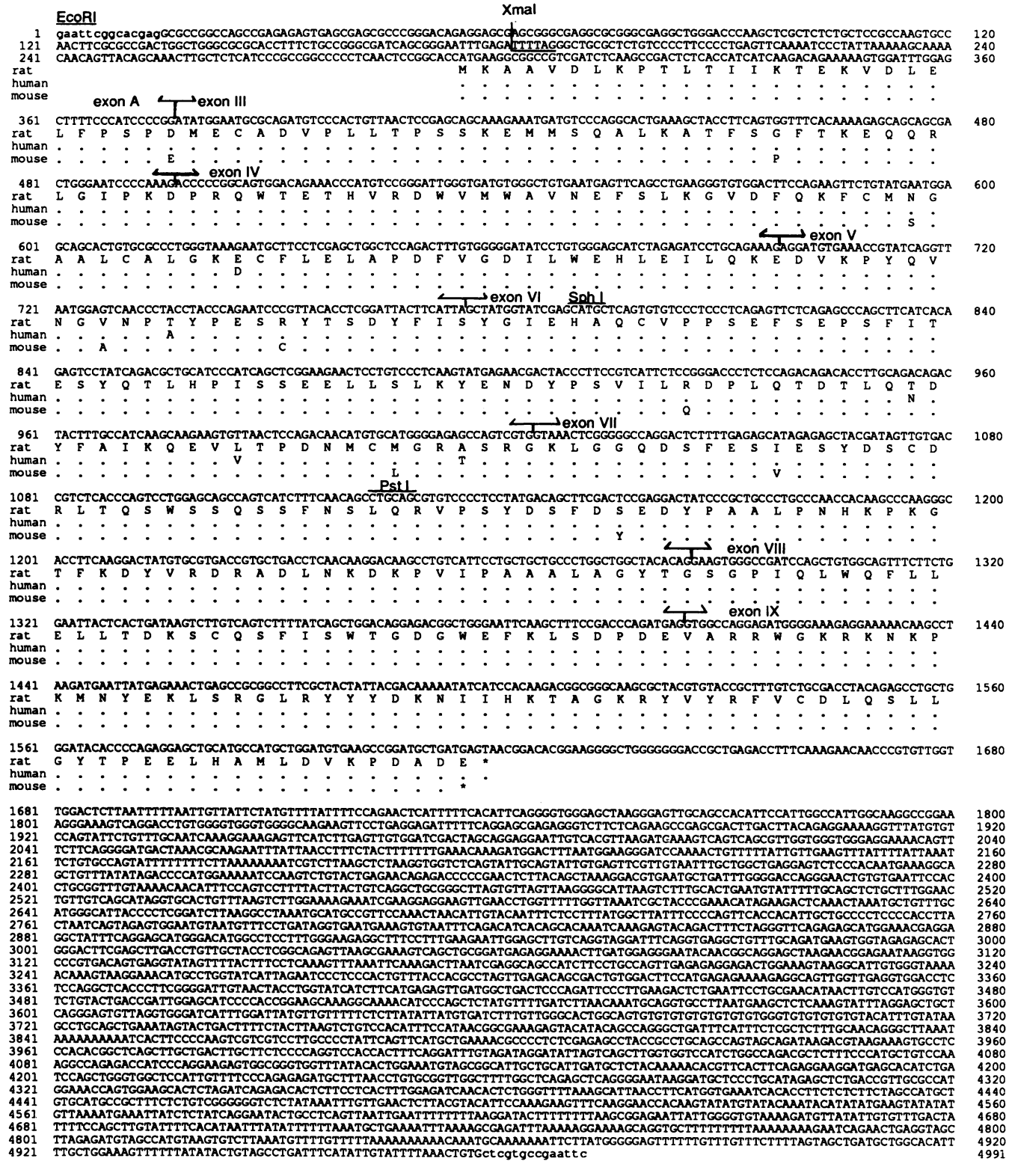

FIG. 2. Nucleotide and deduced amino acid sequences of the *Tpl-1/Ets-1* pRCT14a cDNA clone. The differences between the 441-amino-acid open reading frame and the human and mouse Ets-1 protein are highlighted. Exon boundaries, marked by arrows, and exon nomenclature are those used in references 12 and 33. The sequence of the *Eco*RI linkers used for cDNA library construction is written in lowercase type.

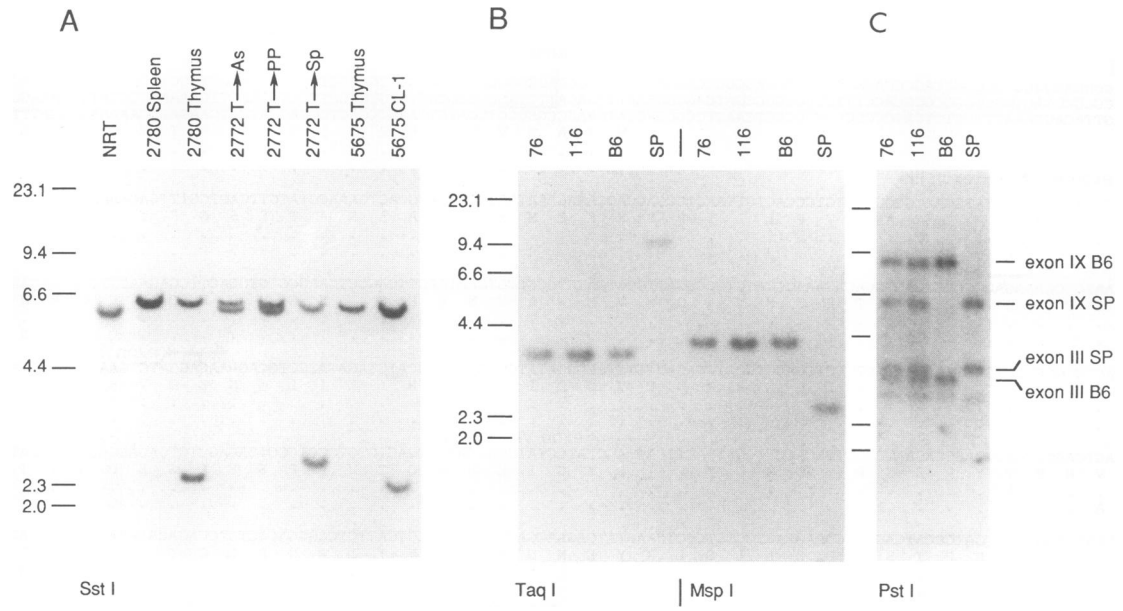

FIG. 3. Genetic mapping of the pRCT14a cDNA clone. Intragenic recombination in *Tpl-1/Ets-1*. (A) Southern blot analysis of *Sst*I-digested DNAs from normal rat thymus (NRT) and MoMuLV-induced primary tumors and cell lines with or without a rearrangement in *Tpl-1*. The *Eco*RI-*Xma*I probe derived from the 5′ untranslated region of pRCT14a detects a rearranged band, due to the insertion of the proviral long terminal repeat *Sst*I site, only in DNA specimens with provirus integration in *Tpl-1*: 2780 Thymus, 2772T→S, and 5675 CL-1 (1) (Fig. 1). The two bands in 2772T→As and 2772T→PP are normal alleles owing to heterozygosity for the polymorphic *Sst*I site (Fig. 1). (B and C) Southern blot analysis of DNA from *Mus musculus* C57BL/6J (B6), *Mus spretus* (SP), and two (*Mus musculus* × *Mus spretus*) × *Mus musculus* interspecific backcross mice (76 and 116), hybridized to the *Tpl-1* probe pSB1 (panel B) and to a mixture of *Ets-1* exon III and IX probes (panel C). Animals 76 and 116 show homozygosity for the *Mus musculus* pSB1 allele and heterozygosity for the *Mus musculus* and *Mus spretus* exon III and IX alleles, owing to a recombination event between the markers pSB1 and exon III. The migration of the exon III and IX *Mus musculus* and *Mus spretus* alleles is indicated. The migration and size (in kilobases) of the markers are shown at the left of each panel. The restriction enzyme used is indicated at the bottom of the panels.

rapid selection. First, we used Northern blot analysis of poly(A)$^+$ RNA to determine the expression of *Tpl-1/Ets-1* in normal rat tissues. This showed that *Tpl-1/Ets-1* is specifically expressed in hematopoietic tissues (spleen and thymus), giving rise to two mRNA transcripts, of 5.5 and 2.2 kb (Fig. 4A). Subsequently, poly(A)$^+$ RNA extracted from six MoMuLV-induced T-cell lymphoma lines, including 2772T→As and 2772T→Ln→Ln, which have a wild-type *Tpl-1* allele, and 2772T→S, harboring a provirus in *Tpl-1*, was hybridized to the pSB8 probe. To determine the relative amount of RNA per lane, we hybridized the same filters to a cDNA clone of the gene encoding the ribosomal protein L32 (RPL32) (17). The intensity of the bands was quantitated with a β scanner. The appropriate ratios between the 5.5- and the 2.2-kb *Ets-1* transcripts and the RPL32 were calculated. The results revealed that provirus insertion is associated with a modest enhancement of the steady-state level of *Ets-1* mRNA (Fig. 4B and C; Table 1).

We then examined the structural differences between the 5.5- and 2.2-kb *Ets-1* mRNA transcripts. Poly(A)$^+$ RNA, extracted from a MoMuLV-induced T-cell lymphoma line derived from tumor 6889, was size fractionated in a sucrose gradient (17), and the fraction between 2 and 3 kb was used to construct a cDNA library, which was screened with the pSB8 probe. Six clones of approximately 2.1 kb were isolated, and their ends were sequenced and aligned with the 5-kb pRCT14a clone. The 3′ ends of all six clones were mapped in a region between nucleotides 2167 and 2198 (Fig. 5A), suggesting that the difference between the 5.5- and 2.2-kb mRNAs is the result of differential polyadenylation. To test this hypothesis, we hybridized Northern blots of poly(A)$^+$ RNA from 2772 cells, with or without a provirus in *Tpl-1*, to probes from either side of the region defined by the 3′ ends of the six clones. This showed that probe A, extending between nucleotides 1587 and 2118, detects both mRNA transcripts, whereas probe B, extending between nucleotides 2259 and 2618, detects only the 5.5-kb mRNA (Fig. 5B). Therefore, the two mRNA transcripts are indeed due to differential polyadenylation. The polyadenylation site responsible for the 2.2-kb mRNA transcript lacks a conventional polyadenylation signal (AAUAAA). To determine whether provirus insertion affected the frequency of transcripts arising by differential polyadenylation, we examined their ratio in 2772 cells with or without a provirus in *Tpl-1*. Quantitation with a β scanner showed that the ratio between the 5.5- and 2.2-kb transcripts (2.1 to 2.4) is not significantly affected by provirus integration (Fig. 5B; Table 1).

The 5′ region of the *Tpl-1/Ets-1* mRNA could theoretically be altered, following provirus insertion in this locus, as a result of promoter insertion or alternate promoter usage. Because of the potential effects of the 5′ region on the efficiency of mRNA translation, we proceeded to map the sites of *Ets-1* transcriptional initiation in normal thymocytes and in the tumor cell line 2780, carrying a provirus in the *Tpl-1* locus. This was done by primer extension with the oligonucleotide primers PT194 and PT265, which are complementary to sequences in exon A (see Fig. 7). To precisely map the sites of transcriptional initiation, we electrophoresed the primer extension products in parallel with the products of sequencing reactions carried out on genomic *Tpl-1* clones with the same oligonucleotide primers. The results shown in Fig. 6 revealed that transcriptional

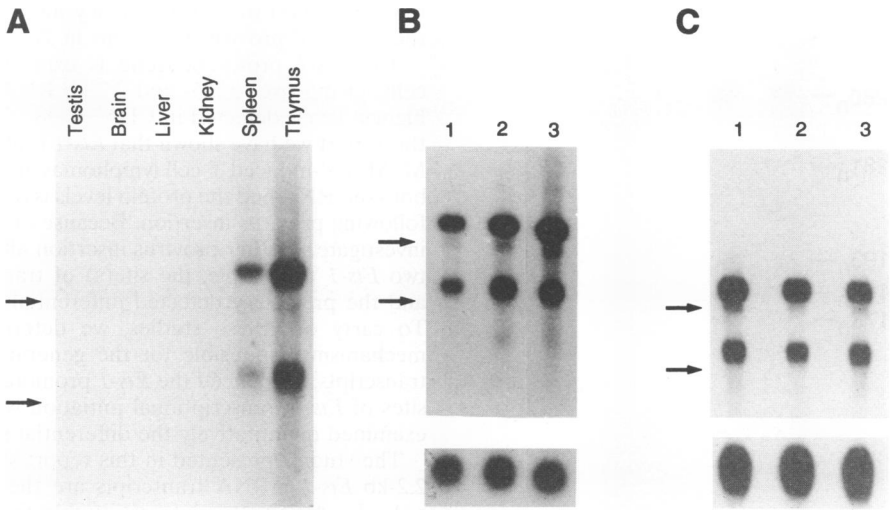

FIG. 4. *Ets-1* expression in normal rat tissues and in MoMuLV-induced T-cell lymphomas. (A) Poly(A)$^+$ RNA extracted from normal rat tissues was electrophoresed in formaldehyde-agarose gels, transferred to nylon membranes, and hybridized to pSB8. Two transcripts of approximately 5.5 and 2.2 kb were detected in the spleen and thymus. No detectable expression was found in the testes, brain, or kidneys. (B) Poly(A)$^+$ RNA extracted from three MoMuLV-induced T-cell lymphomas was electrophoresed in formaldehyde-agarose gels, transferred to nylon membranes, and hybridized to pSB8 (upper panel) and, as a control for the amount of RNA, to the ribosomal protein L32 gene (lower panel). Lanes: 1, LE3Sp Cl1; 2, LE3Sp Cl2; 3, 6890. (C) Poly(A)$^+$ RNA extracted from 2772T→S (lane 1), 2772T→As (lane 2), and 2772T→Ln→Ln (lane 3) was analyzed as in panel B. The cell line 2772T→S, harboring a provirus insertion in *Tpl-1/Ets-1*, shows a slightly higher level of *Ets-1* mRNA expression than do 2272T→As and 2772T→Ln→Ln, which have a wild-type *Tpl-1/Ets-1* allele. Arrows indicate the migration of the 28S and 18S rRNAs.

initiation in the *Tpl-1/Ets-1* promoter is independent of provirus insertion. Figure 7 shows a comparison of the human and rat *Ets-1* promoter-enhancer regions. Portions of these regions are conserved between the two species (12). However, none of the known putative transcription factor-binding sites described for the human *Ets-1* gene is completely conserved in the rat gene (12). The level of Ets-1 protein expression is enhanced only modestly following provirus insertion and correlates with the slightly increased levels of RNA (Fig. 8).

Earlier studies had shown that exons IV and VII of the human *Ets-1* gene undergo alternative splicing (12, 21). To test whether exon VII of the rat *Ets-1* gene is also alternatively spliced and whether provirus insertion affects the splicing frequency, we performed a quantitative RNase protection assay. A 334-bp *Sph*I-*Pst*I fragment spanning exons VI and VII (Fig. 2) was subcloned in pGEM3Z. Following linearization with *Hin*dIII and in vitro transcription with T7 RNA polymerase, we generated a 382-base riboprobe, which included vector sequences. Following hybridization to cellular RNA and RNase A digestion in all tested specimens, the riboprobe was degraded into a 334- and a 231-base fragment corresponding to the unspliced and spliced *Ets-1* mRNAs, respectively (Fig. 9A). The intensity of the bands was quantitated with a β scanner,

TABLE 1. Quantitation of the *Ets-1* RNA transcripts in 2772 cells with or without a provirus in the *Tpl-1* locus, and ratio between the 5.5- and 2.2-kb *Ets-1* transcripts

Sample	Activity (cpm) of band:			Ratio of cpm values for:		
	5.5 kb	2.2 kb	RPL32	5.5 kb/ RPL32	2.2 kb/ RPL32	5.5 kb/ 2.2 kb
2772T→S	12,416	5,122	85,359	0.145	0.060	2.417
2772T→As	7,254	2,786	94,930	0.076	0.029	2.621
2772T→Ln→Ln	9,583	4,456	80,491	0.119	0.055	2.164

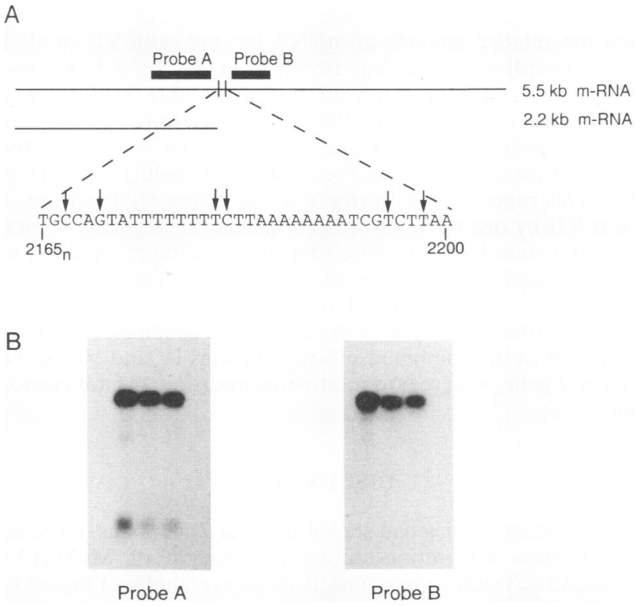

FIG. 5. Differential polyadenylation of the rat *Ets-1* gene; structure of the 5.5- and 2.2-kb transcripts. (A) Mapping of the 3′ ends of six independent *Ets-1* cDNA clones of approximately 2.1 kb, isolated from a size-selected cDNA library, on the sequence of the 5-kb pRCT14a cDNA clone. The transcription end sites of the six clones cluster within a 32-bp region. A schematic representation of the structures of the 5.5- and 2.2-kb rat *Ets-1* mRNAs is shown, along with the origin of probes A and B (see text). (B) Poly(A)$^+$ RNA extracted from three Mo MuLV-induced T-cell lymphoma lines (from left to right, 2772T→S, 2772T→As, and 2772T→Ln→Ln) was electrophoresed in formaldehyde-agarose gels, transferred to nylon membranes, and hybridized to probe A (left panel) and probe B (right panel). Probe A detects both the 5.5- and 2.2-kb mRNAs; probe B hybridizes only to the 5.5-kb mRNA.

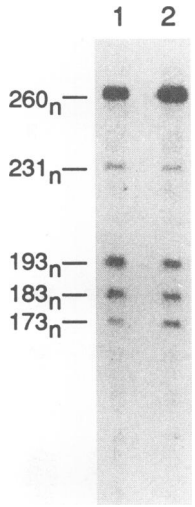

FIG. 6. Primer extension analysis of the rat *Ets-1* mRNA. Primer PT265, which is complementary to a sequence in exon A (see Fig. 7), was hybridized to RNA extracted from normal rat thymus (lane 2) and the 2780 lymphoma line harboring a provirus in *Tpl-1*/*Ets-1* (lane 1). The primer was extended with reverse transcriptase. Five bands of 260, 231, 193, 183, and 173 bases, corresponding to major sites of transcriptional initiation, were detected in both RNA samples. Similar results were obtained with the primer PT194, which is complementary to a sequence 90 bp 3′ of the 5′ end of the pRCT14a cDNA clone (see Fig. 7).

and the relative amount of mRNA lacking exon VII in all T cells, regardless of provirus insertion in the *Tpl-1* locus, was found to be approximately 15 to 26% (Table 2). Sequence analysis of exon VII and the flanking introns revealed an evolutionarily conserved inverted repeat which is present at the 5′ end of exon VII and the 3′ end of the preceding intron (Fig. 9B). This repeat may contribute to the differential splicing of exon VII by one of two potential mechanisms: (i) the formation of a stem-loop structure that prevents the recognition of the overlapping splicing signals or (ii) the binding of a protein that inhibits splicing (Fig. 9C).

A quantitative analysis of the alternative splicing of exon IV, as well as of the combined splicing of exons IV and VII of the rat *Ets-1* gene, with regard to provirus insertion was not carried out.

DISCUSSION

Our earlier studies had shown that the *Tpl-1* locus, targeted for provirus integration during progression of MoMuLV-induced rat T-cell lymphomas, is closely related and linked to the *Ets-1* proto-oncogene (1). In this report we have presented evidence that all the known *Tpl-1* provirus insertions occurred immediately 5′ of the first exon of *Ets-1* and that the earlier uncertainty about the relationship between *Tpl-1* and *Ets-1* was due to the high frequency of meiotic recombination within the site of provirus integrations and exon III. A high frequency of meiotic recombination had previously been shown to occur within the mouse major histocompatibility complex and the pseudo-autosomal region of human chromosome Y (28). Although the molecular mechanism contributing to this phenomenon is not currently known, it should be taken into account during the interpretation of gene-mapping data based on the frequency of genetic recombination. It is intriguing to consider that the site(s) of high-frequency meiotic recombination and the site(s) of provirus insertions in *Tpl-1* overlap.

The *Ets-1* proto-oncogene is expressed in hematopoietic cells, giving rise to 5.5- and 2.2-kb RNA transcripts, with the highest levels detected in $CD4^+$ $CD8^-$ T lymphocytes (5). In this report we have shown that *Ets-1* is also highly expressed in MoMuLV-induced T-cell lymphomas and that its expression at both the RNA and the protein levels is only modestly enhanced following provirus insertion. Because of this, we proceeded to investigate whether provirus insertion affected the ratio of the two *Ets-1* transcripts, the site(s) of transcriptional initiation, and the previously detected differential splicing of exon VII. To carry out these studies, we determined the molecular mechanism responsible for the generation of the two RNA transcripts, sequenced the *Ets-1* promoter region, mapped the sites of *Ets-1* transcriptional initiation within this region, and examined quantitatively the differential splicing of exon VII.

The studies presented in this report show that the 5.5- and 2.2-kb *Ets-1* mRNA transcripts are the result of differential polyadenylation. It is interesting that the polyadenylation site responsible for the 2.2-kb mRNA is not marked by a classical polyadenylation consensus sequence. The sequence closest to the polyadenylation consensus in this region is AACAAA (nucleotides 2094 to 2099). The lack of a strong polyadenylation signal in this region is likely to be the reason that transcription does not terminate reproducibly at this site. Since the 3′ untranslated region contains sequences that may affect the stability of the mRNA, differential polyadenylation may contribute to the regulation of gene expression. Quantitative analysis showed that the ratio of the 5.5- to the 2.2-kb transcript in all tissues expressing *Ets-1* ranges from 2.1 to 2.4 and that it is not affected by provirus insertion in the *Tpl-1* locus.

Provirus insertion in *Tpl-1* could alter the 5′ untranslated region of the *Ets-1* transcripts. This could be the result of either promoter insertion leading to the synthesis of virus-host hybrid mRNA transcripts or provirus insertion-induced differential promoter usage. Our analysis, using primer extension assays, showed that provirus insertion had no effect on the sites of transcriptional initiation, thus excluding any major influences of provirus insertion on translation.

Differential splicing of exon VII may play an important role in the regulation of the transcriptional activity of *Ets-1*. Thus, it has been shown that exon VII contains sites targeted by phosphorylation. Moreover, the Ets-1 protein loses the ability to bind DNA upon phosphorylation of these sites (13, 19). Therefore, differential splicing of exon VII appears to be responsible for the synthesis of an Ets-1 protein product whose DNA-binding activity may not be regulated by phosphorylation. In this paper we have presented evidence that the differential splicing of exon VII may be regulated by a potential sequence-dependent secondary structure at the junction of intron vi and exon VII. Thus, we showed that the sequences at the 5′ end of exon VII are the inverted repeat of the sequences at the 3′ end of the intron. Theoretically this may direct the formation of a stem-loop structure which could interfere with the recognition of the splicing signals at the 5′ end of exon VII. Alternatively, the inverted repeats may form a palindromic binding site for a protein that inhibits splicing. An analogous form of splicing regulation was suggested previously to contribute to the regulation of the differential splicing of exon 6B of the chicken β-tropomyosin gene (15). In this case, secondary structures in *cis* at the intron-exon junction may interact with *trans*-acting factors which compete with the binding of splicing factors (15). Our quantitation of the differential splicing of exon VII revealed that approximately 15 to 26% of the *Ets-1*

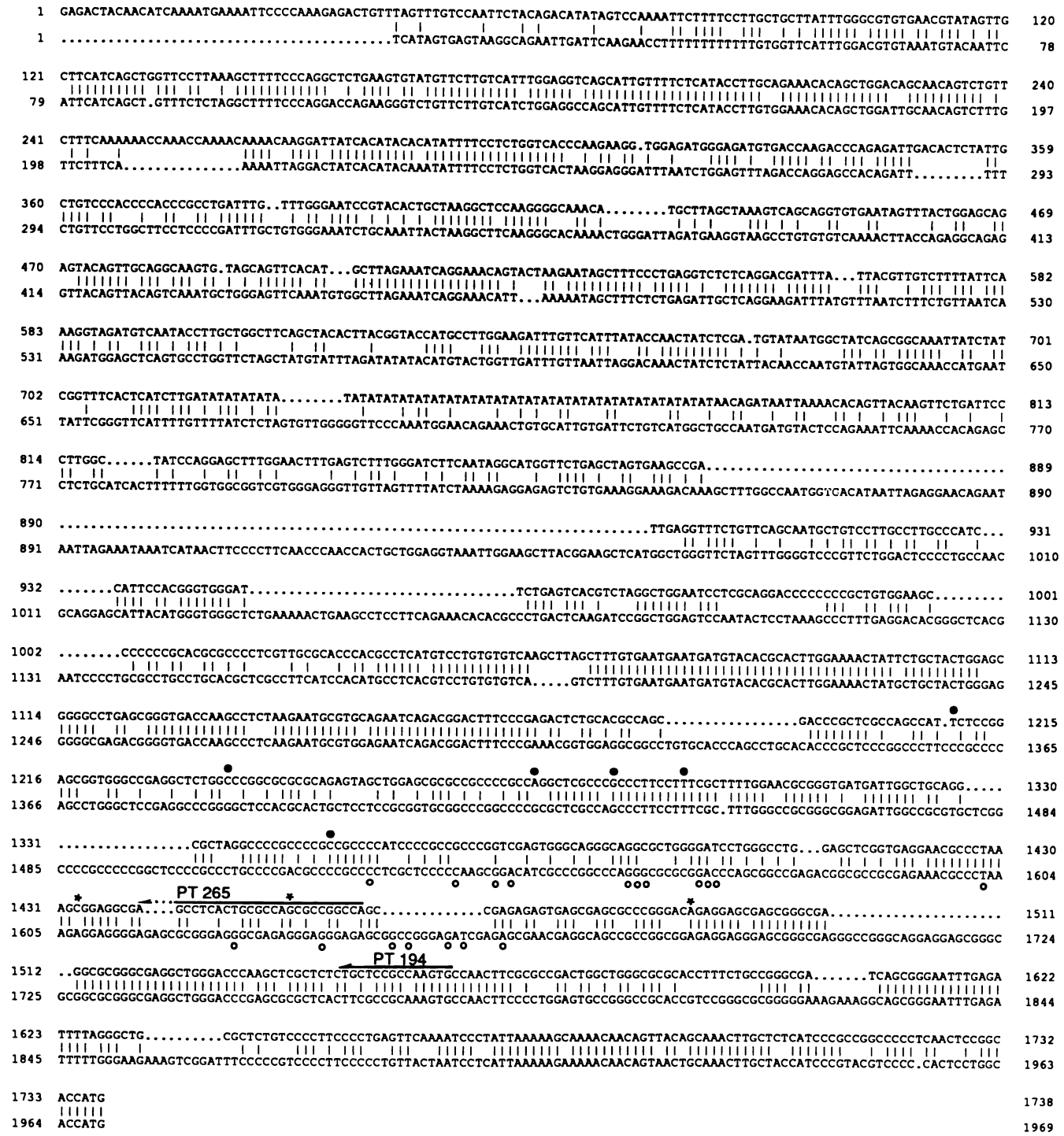

FIG. 7. Promoter region of the rat *Ets-1* gene (upper line) and comparison with the human *Ets-1* promoter (lower line). The sites of transcriptional initiation for the rat and human genes are indicated by solid and open circles, respectively. The asterisks mark sites of initiation corresponding to actual cDNA clones, whose ends were sequenced.

RNA transcripts lack this exon and that provirus insertion does not alter the frequency of differential splicing.

The data discussed in the preceding paragraphs indicate that provirus insertion in the *Tpl-1* locus only modestly affects *Ets-1* expression. Moreover, the *Ets-1* transcripts in tumor cells with a provirus in *Tpl-1* appear to be structurally identical with those detected in normal cells. To reconcile these findings with the strong selection of cells with a provirus in the *Tpl-1* locus, we propose that provirus insertion may exert a subtle effect on the expression of *Ets-1* during cell cycle progression. Stimulation of normal T cells with concanavalin A is associated with a rapid drop in *Ets-1* transcription as well as with the rapid

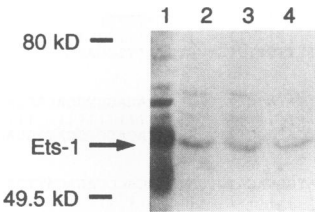

FIG. 8. Ets-1 protein expression in 2772 cell lines. Total protein (75 μg) was separated by SDS-PAGE (10% polyacrylamide), transferred to a polyvinylidene difluoride membrane by electroblotting, and probed with an anti-Ets-1 antibody. The signal was detected by chemiluminescence and quantitated with an image analyzer. The cell line 2772T→S (lane 2) shows slightly higher Ets-1 expression than do 2772T→As (lane 3) and 2772T→Ln→Ln (lane 4): 62,467 counts versus 48,520 and 36,266 counts, respectively. Lane 1 contains Ets-1 protein expressed in Sf9 insect cells infected with a baculovirus construct. The sizes of the markers are shown in kilodaltons.

phosphorylation and degradation of the Ets-1 protein product. This suggests that *Ets-1* may interfere with the transition from G_0 to G_1 (6, 20). Continued stimulation of the cells with concanavalin A, however, is associated with a slow increase of the steady-state levels of *Ets-1* RNA transcripts, suggesting that *Ets-1* may contribute to cell cycle progression in cycling cells (22). Although it is not currently known whether normal cycling cells have cycling levels of *Ets-1*, these observations suggest that provirus insertion may be responsible for the expression of continuously high levels of *Ets-1* RNA during cell cycle progression. This, in turn, may promote the growth of cycling cells or may prevent their exit from the cell cycle.

It is also conceivable that, in addition to the modest effect on *Ets-1*, provirus insertion in *Tpl-1* could affect the expression of another gene, located upstream from the cluster of integrated proviruses. We analyzed genomic clones spanning approximately 18 kb upstream from the site of integration but failed to detect expressed sequences (3a). However, since provirus integration may lead to the enhanced expression of a gene located as far as 300 kb away (29), the possibility that a gene

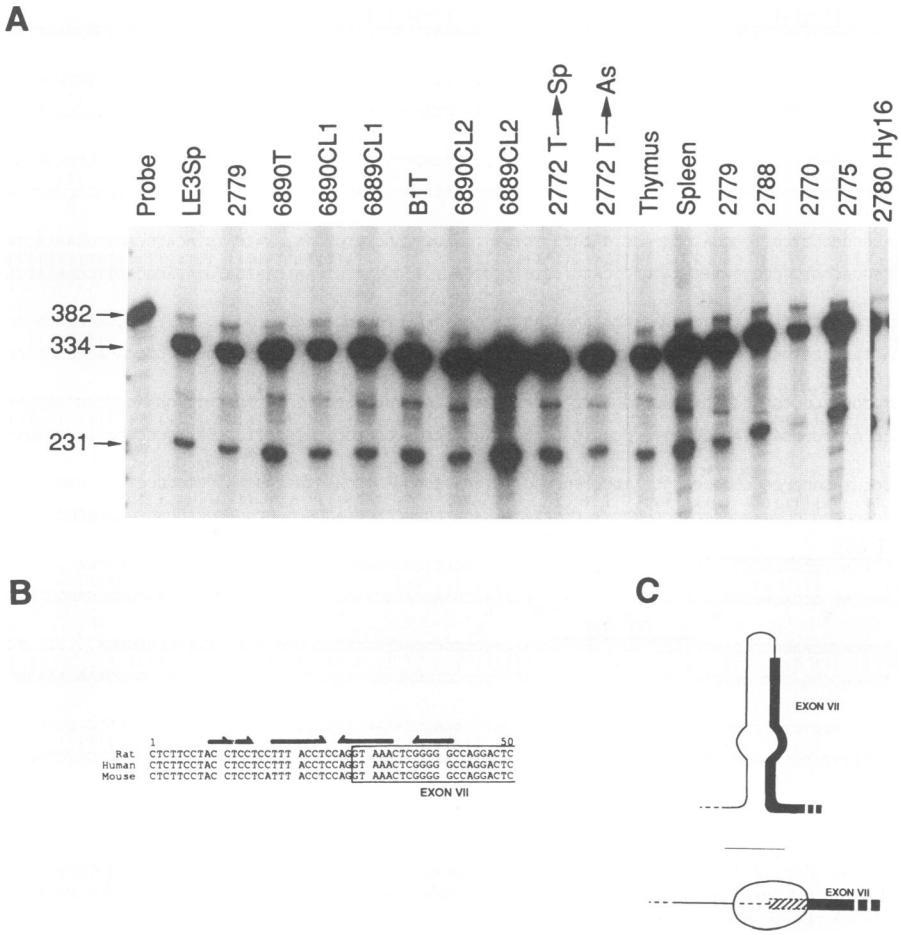

FIG. 9. Alternative splicing of exon VII of the rat *Ets-1* gene. (A) RNase protection assay of exon VII alternative splicing in normal rat tissues and in MoMuLV-induced T-cell lymphoma specimens. A 382-base riboprobe spanning exons VI and VII of the *Ets-1* cDNA and also containing 48 bases of plasmid sequences is degraded in all the specimens to a 334- and a 231-base fragment corresponding to the unspliced *Ets-1* mRNA and to an mRNA lacking exon VII, respectively. No signal was detected in the mouse-rat hybrid cell line 2780Hy16, which has a homozygous deletion of the rat *Ets-1* chromosomes (negative control). (B) Inverted repeats, whose direction is indicated by arrows, surround the exon VII splice acceptor site. The repeats are conserved in the rat, human, and mouse *Ets-1* genes. (C) Hypothetical models of the function of the inverted repeats in the regulation of alternative splicing of *Ets-1* exon VII. The repeats could generate a stem-loop structure (upper panel); alternatively, they could represent a palindromic binding site for a splicing factor (lower panel). In both cases the splice acceptor site of exon VII would not be accessible to the splicing machinery.

TABLE 2. Alternative splicing of rat *Ets-1* exon VII as shown by quantitation by RNase protection[a]

Sample	Activity (cpm) (%) of:	
	334-bp band	231-bp band
LE3Sp	27,102 (79.3)	5,152 (20.7)
2779	25,381 (80.0)	4,618 (20.0)
6890T	48,828 (78.5)	9,726 (21.5)
6890C11	26,439 (74.1)	6,712 (25.9)
6889C11	49,934 (83.0)	7,433 (17.0)
B1T	51,819 (78.9)	10,043 (21.1)
6890C12	37,270 (77.2)	8,019 (22.8)
6889C12	114,103 (75.7)	26,697 (24.3)
2772T→Sp	47,040 (78.8)	9,191 (21.2)
2772T→As	35,438 (80.8)	6,158 (19.2)
Thymus	23,260 (78.4)	4,663 (21.6)
Spleen	67,848 (84.3)	9,152 (15.7)
2779	42,587 (85.1)	5,446 (14.9)
2780	37,018 (81.1)	6,284 (18.9)
2770	11,327 (76.6)	2,515 (23.4)
2775	45,790 (81.1)	7,751 (18.9)

[a] Since labeling was done with [α-^{32}P]CTP, in order to calculate the percentage of the transcripts with and without exon VII, the cpm values of the 334- and 241-bp bands were divided by the number of C residues present in each band: 103 and 75, respectively.

other than *Ets-1* is activated by provirus insertion in *Tpl-1* cannot be ruled out.

ACKNOWLEDGMENTS

This research was supported by CTR grant 2976 and ACS grant MV-524. Additional support was provided by Public Health Service grant RR-05539, an appropriation from the Commonwealth of Pennsylvania to the Fox Chase Cancer Center, and by the National Cancer Institute under contract NO1-CO-74101 with ABL. A.B. was a Fellow of the Lawrence Greenwald Foundation for Leukemia and Lymphoma research; he is currently a Fellow of the Italian Association for Cancer Research (AIRC). C.P. was a fellow of The Leukemia Society of America Inc.

We are grateful to Arun Seth and Takis Papas for the gift of the baculovirus-expressed Ets-1 protein. We thank Deborah Gilbert for expert technical assistance and Pat Bateman for secretarial assistance.

REFERENCES

1. **Bear, S. E., A. Bellacosa, P. A. Lazo, N. A. Jenkins, N. G. Copeland, C. Hanson, G. Levan, and P. N. Tsichlis.** 1989. Provirus insertion in *Tpl*-1, an *Ets*-1 related oncogene is associated with tumor progression in MoMuLV-induced rat thymic lymphomas. Proc. Natl. Acad. Sci. USA **86**:7495–7499.
2. **Bellacosa, A., T. F. Franke, M. E. Gonzalez-Portal, K. Datta, T. Taguchi, J. Gardner, J. Q. Cheng, J. R. Testa, and P. N. Tsichlis.** 1993. Structure, expression and chromosomal mapping of c-*akt*: relationship to v-*akt* and its implications. Oncogene **8**:745–754.
3. **Bellacosa, A., P. A. Lazo, S. E. Bear, and P. N. Tsichlis.** 1991. The rat leukocyte antigen MRC OX-44 is a member of a new family of cell surface proteins which appear to be involved in growth regulation. Mol. Cell. Biol. **11**:2864–2872.

3a. **Bellacosa, A., and P. N. Tsichlis.** Unpublished data.

4. **Berger, S. L.** 1987. Preparation and characterization of RNA: overview. Methods Enzymol. **152**:215–227.
5. **Bhat, N. K., K. L. Komschlies, S. Fujiwara, R. J. Fisher, B. J. Mathieson, T. A. Gregorio, H. A. Young, J. W. Kasik, K. Ozato, and T. S. Papas.** 1989. Expression of *ets* genes in mouse thymocyte subsets and T cells. J. Immunol. **142**:672–678.
6. **Bhat, N. K., C. B. Thompson, T. Lindsten, C. H. June, S. Fujiwara, S. Koizumi, R. G. Fisher, and T. S. Papas.** 1990. Reciprocal expression of human *ETS1* and *ETS2* genes during T-cell activation: regulatory role for the protooncogene *ETS1*. Proc. Natl. Acad. Sci. USA **87**:3723–3727.
7. **Devereux, J., P. Haeberli, and O. Smithies.** 1984. A comprehensive set of sequence analysis programs for the VAX. Nucleic Acids Res. **12**:387–395.
8. **Gubler, U., and B. J. Hoffman.** 1983. A simple and very efficient method for generating cDNA libraries. Gene **25**:263–269.
9. **Gunther, C. V., J. A. Nye, R. S. Bryner, and B. J. Graves.** 1990. Sequence-specific DNA binding of the proto-oncoprotein ets-1 defines a transcriptional activator sequence within the long terminal repeat of the Moloney sarcoma virus. Genes Dev. **4**:667–679.
10. **Henikoff, S.** 1984. Unidirectional digestion with exonuclease III creates targeted breakpoints for DNA sequencing. Gene **28**:351–359.
11. **Jacobson, A.** 1987. Purification and fractionation of poly(A)$^+$ RNA. Methods Enzymol. **152**:254–261.
12. **Jorcyk, C. L., D. K. Watson, G. J. Mavrothalassitis, and T. S. Papas.** 1991. The human *ETS1* gene: genomic structure, promoter characterization and alternative splicing. Oncogene **6**:523–532.
13. **Koizumi, S., R. J. Fisher, S. Fujiwara, C. Jorcyk, N. K. Bhat, A. Seth, and T. S. Papas.** 1990. Isoforms of the human *ets*-1 protein: generation by alternative splicing and differential phosphorylation. Oncogene **5**:675–681.
14. **Lazo, P. A., A. J. P. Klein-Szanto, and P. N. Tsichlis.** 1990. T-cell lymphoma lines derived from rat thymomas induced by Moloney murine leukemia virus: phenotypic diversity and its implications. J. Virol. **64**:3948–3959.
15. **Libri, D., A. Piseri, and M. Y. Fiszman.** 1991. Tissue-specific splicing in vivo of the β-tropomyosin gene: dependence on an RNA secondary structure. Science **252**:1842–1845.
16. **Lim, H. M., and J. J. Pene.** 1988. Optimal conditions for supercoil DNA sequencing with the *Escherichia coli* DNA polymerase I large fragment. Gene Anal. Tech. **5**:32–39.
17. **Patriotis, C., A. Makris, S. E. Bear, and P. N. Tsichlis.** 1993. Tumor progression locus 2 (*Tpl*-2) encodes a protein kinase involved in the progression of rodent T-cell lymphomas and in T-cell activation. Proc. Natl. Acad. Sci. USA **90**:2251–2255.
18. **Paul, R., S. Schuetze, S. L. Kozak, C. A. Kozak, and D. Kabat.** 1991. The *Sfpi-1* proviral integration site of Friend erythroleukemia encodes the *ets*-related transcription factor Pu.1. J. Virol. **65**:464–467.
19. **Pognonec, P., K. E. Boulukos, R. Bosselut, C. Boyer, A. M. Schmitt-Verhulst, and J. Ghysdael.** 1990. Identification of an Ets1 variant protein unaffected in its chromatin and in vitro DNA binding capacities by T cell antigen receptor triggering and intracellular calcium rises. Oncogene **5**:603–610.
20. **Pognonec, P., K. E. Boulukos, J. C. Gesquiere, D. Stehelin, and J. Ghysdael.** 1988. Mitogenic stimulation of thymocytes results in the calcium-dependent phosphorylation of c-ets-1 proteins. EMBO J. **7**:977–983.
21. **Reddy, E. S., and V. N. Rao.** 1988. Structure, expression and alternative splicing of the human c-*ets*-1 proto-oncogene. Oncogene Res. **3**:239–246.
22. **Reed, J. C., J. D. Alpers, P. C. Nowell, and R. G. Hoover.** 1986. Sequential expression of proto-oncogenes during lectin-stimulated mitogenesis of normal human lymphocytes. Proc. Natl. Acad. Sci. USA **83**:3982–3986.
23. **Reicin, A., J.-Q. Yang, K. B. Marcu, E. Fleissner, C. F. Koehne, and P. V. O'Donnell.** 1986. Deregulation of the c-*myc* oncogene in virus-induced thymic lymphomas of AKR/J mice. Mol. Cell. Biol. **6**:4088–4092.
24. **Saiki, R. K., S. Scharf, F. Faloona, K. B. Mullis, G. T. Horn, H. A. Erlich, and N. Arnheim.** 1985. Enzymatic amplification of β-globin genomic sequences and restriction site analysis for diagnosis of sickle cell anemia. Science **230**:1350–1354.
25. **Sambrook, J., E. F. Fritsch, and T. Maniatis.** 1989. Molecular cloning: a laboratory manual, 2nd ed. Cold Spring Harbor Laboratory, Cold Spring Harbor, N.Y.
26. **Sanger, F., S. Nicklen, and A. R. Coulson.** 1977. DNA sequencing with chain-terminating inhibitors. Proc. Natl. Acad. Sci. USA **74**:5463–5467.
27. **Short, J. M., J. M. Fernandez, J. A. Sorge, and W. D. Huse.** 1988. λZAP: a bacteriophage λ expression vector with in vivo excision properties. Nucleic Acids Res. **16**:7583–7600.
28. **Steinmetz, M., Y. Uematsu, and K. Fischer Lindahl.** 1987.

Hotspots of homologous recombination in mammalian genomes. Trends Genet. **3:**7–10.

29. **Tsichlis, P. N., and P. A. Lazo.** 1991. Virus-host interactions and the pathogenesis of murine and human oncogenic retroviruses. Curr. Top. Microbiol. Immunol. **171:**95–179.
30. **Tsichlis, P. N., P. G. Strauss, and L. F. Fu.** 1983. A common region of proviral DNA integration in MoMuLV-induced rat thymic lymphomas. Nature (London) **302:**445–449.
31. **Tsichlis, P. N., P. G. Strauss, and M. A. Lohse.** 1985. Concerted DNA rearrangements in Moloney murine leukemia virus-induced thymomas: a potential synergistic relationship in oncogenesis. J. Virol. **56:**258–267.
32. **Watson, D. K., M. J. McWilliams, P. Lapis, J. A. Lautenberger, C. W. Schweinfest, and T. S. Papas.** 1988. Mammalian *ets-1* and *ets-2* genes encode highly conserved proteins. Proc. Natl. Acad. Sci. USA **85:**7862–7866.
33. **Watson, D. K., M. J. McWilliams, and T. S. Papas.** 1988. Molecular organization of the chicken *ets* locus. Virology **164:**99–105.